Neurobiology of Disease 96 (2016) 95–104

Contents lists available at ScienceDirect

Neurobiology of Disease

journal homepage: www.elsevier.com/locate/ynbdi

An animal model of Miller Fisher syndrome: Mitochondrial hydrogen peroxide is produced by the autoimmune attack of nerve terminals and activates Schwann cells

Umberto Rodella [a], Michele Scorzeto [a], Elisa Duregotti [a], Samuele Negro [a], Bryan C. Dickinson [b], Christopher J. Chang [c,d], Nobuhiro Yuki [e], Michela Rigoni [a,*], Cesare Montecucco [a,f,*]

[a] Department of Biomedical Sciences, University of Padua, Padua, Italy
[b] Department of Chemistry, The University of Chicago, Chicago, IL, USA
[c] Department of Chemistry and Molecular and Cell Biology, University of California, Berkeley, CA, USA
[d] Howard Hughes Medical Institute, University of California, Berkeley, CA, USA
[e] Department of Neurology, Mishima Hospital, Niigata, Japan
[f] CNR Institute of Neuroscience, Padua, Italy

ARTICLE INFO

Article history:
Received 29 June 2016
Revised 30 August 2016
Accepted 1 September 2016
Available online 03 September 2016

Keywords:
Miller Fisher syndrome
Neuromuscular junction
Hydrogen peroxide
ERK1/2
Schwann cells

ABSTRACT

The neuromuscular junction is a tripartite synapse composed of the presynaptic nerve terminal, the muscle and perisynaptic Schwann cells. Its functionality is essential for the execution of body movements and is compromised in a number of disorders, including Miller Fisher syndrome, a variant of Guillain-Barré syndrome: this autoimmune peripheral neuropathy is triggered by autoantibodies specific for the polysialogangliosides GQ1b and GT1a present in motor axon terminals, including those innervating ocular muscles, and in sensory neurons. Their binding to the presynaptic membrane activates the complement cascade, leading to a nerve degeneration that resembles that caused by some animal presynaptic neurotoxins.

Here we have studied the intra- and inter-cellular signaling triggered by the binding and complement activation of a mouse monoclonal anti-GQ1b/GT1a antibody to primary cultures of spinal cord motor neurons and cerebellar granular neurons. We found that a membrane attack complex is rapidly assembled following antibody binding, leading to calcium accumulation, which affects mitochondrial functionality. Consequently, using fluorescent probes specific for mitochondrial hydrogen peroxide, we found that this reactive oxygen species is rapidly produced by mitochondria of damaged neurons, and that it triggers the activation of the MAP kinase pathway in Schwann cells.

These results throw light on the molecular and cellular pathogenesis of Miller Fisher syndrome, and may well be relevant to other pathologies of the motor axon terminals, including some subtypes of the Guillain Barré syndrome.

1. Introduction

Miller Fisher syndrome (MFS) is a peripheral neuropathy characterized by ophthalmoplegia, ataxia, and areflexia (Fisher, 1956). The pathogenic factors are autoantibodies specific for the oligosaccharide portion of specific polysialogangliosides, mainly GQ1b and GT1a (Chiba et al., 1993). These antibodies form during the immune response against some viral or bacterial infections, and bind microbial antigens that mimic nerve polysialogangliosides, highly enriched in murine nerve terminals in the diaphragm (Yuki et al., 1994; Goodyear et al., 1999). Anti-GQ1b/GT1a autoantibodies are also associated with incomplete forms of MFS, including an acute ophthalmoparesis without ataxia, an acute ataxic neuropathy without ophthalmoplegia, and its central nervous system subtype termed Bickerstaff brain-stem encephalitis (Wakerley et al., 2014). All these syndromes benefit from plasmapheresis and intravenous immunoglobulin administration and are reversible.

The common pathogenic step is the binding of autoantibodies to presynaptic neuronal membranes enriched in the polysialogangliosides GQ1b and GT1a, and the ensuing recruitment of complement (O'Hanlon et al., 2001). The activated complement forms a transmembrane pore named membrane attack complex (MAC), allowing the rapid entry of Ca^{2+} which triggers degeneration of the axon terminals (Orrenius et al., 2003; Bano and Nicotera, 2007; Rupp et al., 2012). This form of neurodegeneration appears to be confined to the axon terminal of peripheral neurons.

* Corresponding authors.
E-mail addresses: rigonimic@gmail.com (M. Rigoni), cesare.montecucco@gmail.com (C. Montecucco).
Available online on ScienceDirect (www.sciencedirect.com).

http://dx.doi.org/10.1016/j.nbd.2016.09.005

In many respects this autoimmune pathology resembles the one caused by animal presynaptic neurotoxins, which cause a rapid uptake of Ca^{2+} ions within the motor axon terminal. Experiments performed in *ex-vivo* murine nerve-muscle preparations show that the antibody *plus* complement complex bound to the presynaptic membrane damages the neuromuscular junction (NMJ) very similarly both morphologically and electrophysiologically to α-latrotoxin (Halstead et al., 2004), with paralysis and degeneration of nerve endings. In mice the disease is very similar to the human pathology with reversible paralysis of the NMJ, but with a more rapid time course. Complete regeneration is usually achieved within five days, as it occurs following α-latrotoxin poisoning (Duregotti et al., 2015).

The molecular and cellular events involved in the reversible degeneration of motor axon terminals by anti-ganglioside antibodies *plus* complement are ill-known, and are the focus of the present study. Here, we have used a mouse monoclonal anti-GQ1b/GT1a antibody, previously characterized as the MFS inducer (Koga et al., 2005), and have studied the intra- and intercellular signaling events triggered by the anti-ganglioside antibody *plus* complement complex at the murine NMJ, in two types of primary cultured neurons, and in co-cultures of neurons with Schwann cells (SCs).

2. Materials & methods

2.1. Chemicals

The mouse monoclonal antibody (FS3, isotype IgG2b-κ) was previously characterized (Koga et al., 2005). For immunization mice were inoculated with a heat-killed *C. jejuni* lysate, the infectious agent frequently associated with MFS. FS3 recognizes gangliosides GQ1b and GT1a, the latter being identical to GQ1b except for one sialic acid residue less. Normal human serum (NHS) from a pool of human healthy males AB plasma (Sigma-Aldrich #H4522, lot #SLBG2952V) was employed as a source of complement. Unless otherwise stated, all reagents were purchased from Sigma.

2.2. Mice

Experiments were performed in Swiss-Webster adult male CD1 mice. All procedures were performed in accordance with the Council Directive 2010/63/EU of the European Parliament and approved by the Italian Ministry of Health.

2.3. NMJ immunohistochemistry

For binding studies whole LAL and EOMs were incubated *ex-vivo* with FS3 10 μg/mL at 10 °C for 15–30 min, then washed, fixed and processed for immunofluorescence (see below).

For MAC deposition analysis FS3 (10 μg) was diluted with NHS 50% (v/v) in 100 μL of physiological saline (0.9% wt/v NaCl in distilled water), and injected s.c. in proximity of LAL muscle of anesthetized CD1 of around 20–25 g; muscles were collected after 2 h. In the case of EOMs, an *ex vivo* incubation was performed (FS3 10 μg/mL + NHS 50% v/v, 1 h at 37 °C). Heat inactivation of NHS (56 °C for 30 min, HI-NHS), or treatment with NHS 50% alone were employed as negative controls.

To define the kinetics of nerve terminal degeneration and regeneration in mice, FS3 (10 μg) was diluted with NHS 50% (v/v) in 100 μL physiological solution, and subcutaneously injected close to LAL muscles, or intramuscularly in the mice hind limb for different time points. Muscles were then fixed in 4% (wt/v) PFA in PBS for 15 min at room temperature, quenched in PBS + 50 mM NH_4Cl, and then permeabilized and saturated in blocking solution: 15% (v/v) goat serum, 2% (wt/v) BSA, 0.25% gelatin, 0.20% (wt/v) glycine, and 0.5% Triton X-100 in PBS 2 h at room temperature. Incubation with the following primary antibodies was carried out for 48–72 h in blocking solution: anti-neurofilaments (mouse monoclonal, anti-NF200, 1:200, Sigma), anti-VAchT (rabbit polyclonal, 1:1000, Synaptic Systems), anti-C5b-9 (rabbit polyclonal, 1:1000, Abcam). Muscles were then washed and incubated with secondary antibodies (Alexa-conjugated, 1:200, Life Technologies). Nuclei were stained with Hoechst. NMJs were identified by Alexa-conjugated α-bungarotoxin (α-BTx). Images were collected with a Leica SP5 confocal microscope equipped with a 63× HCX PL APO NA 1.4.

2.4. Electrophysiological recordings

Mice were sacrificed at scheduled times by anaesthetic overdose followed by cervical dislocation, soleus muscles dissected and subjected to electrophysiological measurements. Three mice were used for each condition at each time point. Electrophysiological recordings were performed in oxygenated Krebs-Ringer solution on sham or FS3 + NHS injected soleus muscles using intracellular glass microelectrodes (WPI, Germany) filled with one part of 3 M KCl and two parts of 3 M CH_3COOK.

Evoked neurotransmitter release was recorded in current-clamp mode, and resting membrane potential was adjusted with current injection to −70 mV. Evoked junction potentials (EJPs) were elicited by supramaximal nerve stimulation at 0.5 Hz using a suction microelectrode connected to a S88 stimulator (Grass, USA). To prevent muscle contraction, samples were incubated for 10 min with 1 μM μ-Conotoxin GIIIB (Alomone, Israel). Signals were amplified with intracellular bridge mode amplifier (BA-01×, NPI, Germany), sampled using a digital interface (NI PCI-6221, National Instruments, USA) and recorded by means of electrophysiological software (WinEDR, Strathclyde University). EJPs measurements were carried out with Clampfit software (Molecular Devices, USA), statistical analysis with Prism (GraphPad Software, USA).

2.5. Primary cell cultures and co-cultures

Rat cerebellar granular neurons (CGNs), spinal cord motor neurons (SCMNs), primary SCs and their relative co-cultures were prepared as described previously (Rigoni et al., 2007; Duregotti et al., 2015).

2.6. Immunofluorescence

For binding experiments CGNs (6 DIV, *days in culture*) or SCMNs (4–5 DIV), plated onto 35-mm dishes or 24 well-plates, were exposed to FS3 0.1 μg/mL at 16 °C for 20 min in Krebs Ringer buffer for CGNs (KRH: Hepes 25 mM at pH 7.4, NaCl 124 mM, KCl 5 mM, $MgSO_4$ 1.25 mM, $CaCl_2$ 1.25 mM, KH_2PO_4 1.25 mM, glucose 8 mM), and E4 medium for SCMNs (E4: 120 mM NaCl, 3 mM KCl, 2 mM $MgCl_2$, 2 mM $CaCl_2$, 10 mM glucose, and 10 mM Hepes, pH 7.4). Cells then washed, and subjected to immunofluorescence (see below).

For studies on MAC deposition and *bulge* characterization neurons were exposed to FS3 0.1 μg/mL + NHS 0.5% (v/v) at 37 °C for 20 min.

Following treatments cells were washed, fixed for 10 min in 4% (wt/v) paraformaldehyde (PFA) in PBS and quenched (0.38% glycine, 50 mM NH_4Cl in PBS) at room temperature. Cells were permeabilized and saturated in buffer A (20 mM PIPES, 137 mM NaCl, 2.7 mM KCl, pH 6.8) containing 5% (v/v) goat serum, 50 mM NH_4Cl and 0.5% (wt/v) saponin for 45 min, followed by an overnight incubation in buffer A *plus* 5% goat serum and 0.1% (wt/v) saponin with anti-C5b-9 (rabbit polyclonal, 1:5000, Abcam), or VAMP2 (1:500, Rossetto et al., 1996) primary antibodies. After washes, samples were incubated with the correspondent secondary antibodies (Alexa-conjugated, 1:200; Life Technologies) in buffer A *plus* 5% goat serum and 0.1% (wt/v) saponin for 45 min and washed in buffer A. Nuclei were stained with Hoechst. Coverslips were mounted in ProLong Diamond (Thermo Fisher) and examined by epifluorescence (Leica CTR6000) microscopy.

2.7. Calcium imaging

Primary neurons were loaded for 10 min with the calcium indicator Fluo-4 AM (4 μM, Life Technologies), washed and transferred to the stage of an inverted fluorescence microscope (Eclipse-Ti; Nikon Instruments), equipped with the perfect focus system (PFS; Nikon Instruments) and with high numerical aperture oil immersion objectives (60×). Calcium signals were recorded in control samples and in samples exposed to FS3 0.1 μg/mL + NHS 0.5% (v/v) for 20 min with excitation of the fluorophore performed at 465–495 nm by means of an Hg arc lamp (100 W; Nikon). Emitted fluorescence was collected at 515–555 nm. Fluorescence (F) was measured in a selected region of interest (ROI) containing cell cytosol and corrected for background. Measurements were expressed as F/F0 fold increase (%), where F0 represents the fluorescence level at $t = 0$. Images were acquired for 20 min every 20 s.

2.8. Mitochondrial imaging

SCMNs or CGNs were loaded with tetramethylrhodamine methyl ester (TMRM, Life Technologies) 10 nM for 10 min at 37 °C, washed and equilibrated at room temperature for 10 min before FS3 + NHS addition (FS3 0.1 μg/mL + NHS 0.5% (v/v) for 10 min). At the end of each experiment 10 μM carbonylcyanide-*p*-trifluoromethoxyphenyl hydrazone (FCCP), a known mitochondrial electron chain uncoupler, was added as positive control. For mitochondrial morphology studies cells were loaded with Mitotracker Red (Life Technologies) 25 nM for 10 min at 37 °C and then washed prior to image acquisition.

2.9. Hydrogen peroxide detection

Hydrogen peroxide was measured in primary neurons exposed to FS3 0.1 μg/mL + NHS 0.5% (v/v) for 20 min using Mitochondria Peroxy Yellow 1 (MitoPY1) or Peroxyfluor 6 acetoxymethyl ester (PF6-AM), probes specific for mitochondrial and cytoplasmic H_2O_2 detection, respectively (Dickinson and Chang, 2008; Dickinson et al., 2011). Both probes were loaded at 5 μM for 30 min at 37 °C in E4 medium (SCMNs) or KRH (CGNs).

2.10. Western blotting

SCMNs were exposed to FS3 0.1 μg/mL + NHS 0.5% (v/v) for different time points in the presence or absence of catalase (500 U/well), added 5 min before stimulus application and kept throughout the experiment.

Following treatments, samples were lysed in lysis buffer (4% SDS, 0.125 M Tris-HCl, protease inhibitors cocktail (Roche), and phosphatase inhibitor cocktail (Sigma)). Total lysates were loaded on Precast 4–12% SDS-polyacrylamide gels (Life Technologies) and transferred onto nitrocellulose paper in a refrigerated chamber. After saturation, membranes were incubated overnight with a rabbit polyclonal antibody for phospho-p44/42 MAPK (1:1000, Cell Signaling), followed by an anti-rabbit secondary

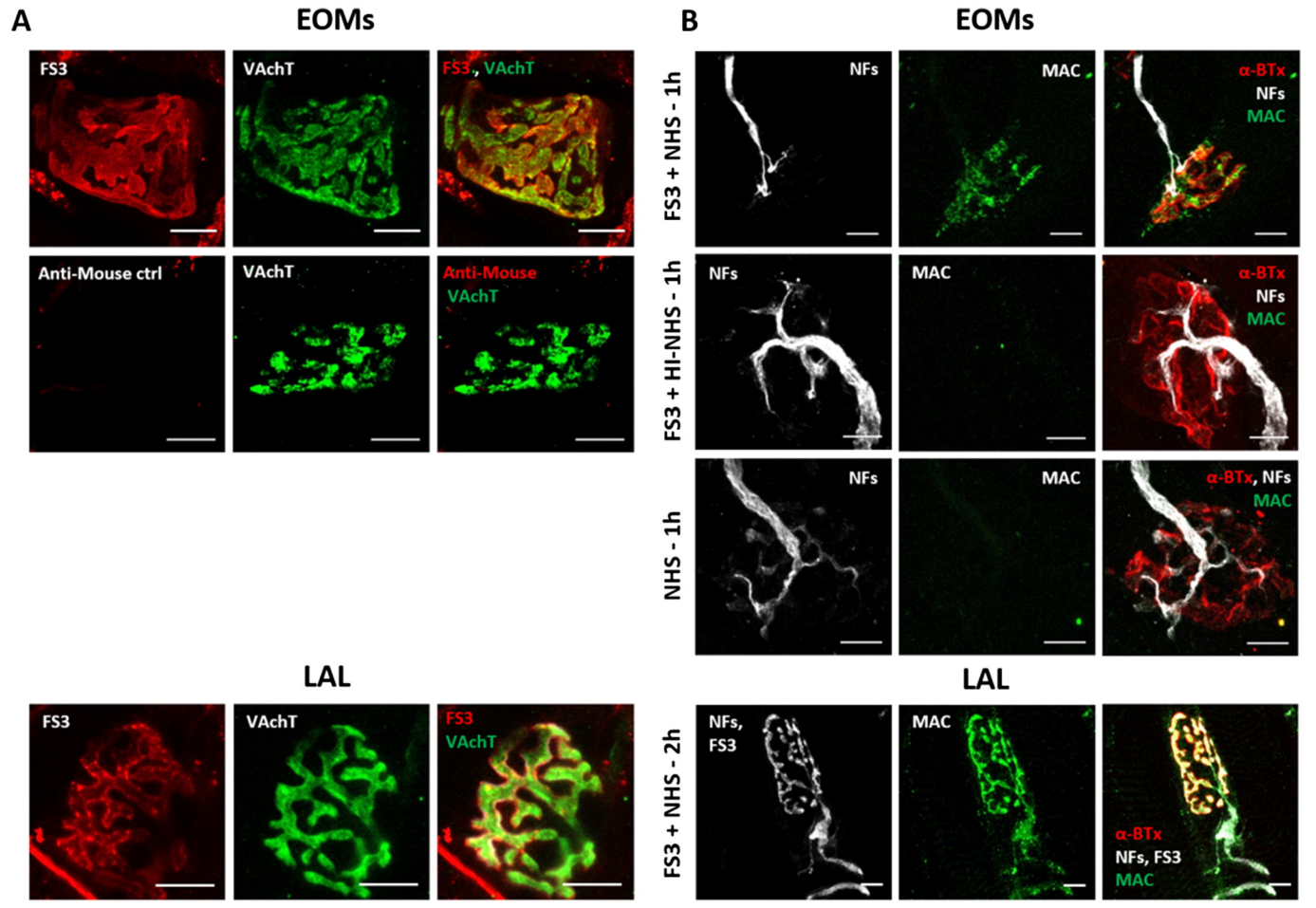

Fig. 1. Anti-GQ1b binding and MAC deposition *in vivo* at murine NMJs. (A) FS3 (*red*) binds to presynaptic nerve terminals of *ex-vivo* preparations of whole EOMs and LAL mice muscles and co-localizes with the presynaptic protein VAchT (*green*). FS3 was detected by an anti-mouse fluorescent secondary antibody. The secondary antibody gave no aspecific signal. (B) FS3 + NHS leads to MAC deposition (*green*) on the neuronal surface of *ex-vivo* treated EOMs and *in vivo* injected LAL muscles. Axon terminals are identified by NF staining (*white*), the postsynaptic element by fluorescent α-BTx (*red*). MAC formation is complement- and FS3-dependent, as no signal is detectable in FS3 + HI-NHS and NHS treated NMJs. Scale bars: 10 μm.

antibody HRP-conjugated (Life Technologies, 1:2000). Chemiluminescence was developed with the Luminata TM Crescendo (Millipore), and emission measured with ChemiDoc XRS (Bio-Rad). For densitometric quantification, the bands of interest were normalized to the housekeeping protein Hsp90 (mouse monoclonal, 1:1000, BD Transduction Laboratories). Band intensities were quantified on the original files with the software Quantity One (Bio-Rad). None of the bands reached saturation.

3. Results

3.1. Anti-GQ1b antibody binds to the neuromuscular junction and triggers a complement-mediated reversible degeneration of motor axon nerve terminals

Fig. 1A shows that FS3 binds specifically to the presynaptic membranes of motor axons innervating mice extra-ocular muscles (EOMs), whose terminals are highly enriched in GQ1b and GT1a gangliosides (Liu et al., 2009), and to the *Levator auris longus* (LAL) muscle which is part of mouse cranial muscles (Angaut-Petit et al., 1987). Presynaptic nerve terminals are identified here by the vesicular acetylcholine transporter (VAchT) staining. FS3, when combined to normal human serum (NHS) as a source of complement (FS3 + NHS), triggers the formation and deposition of the MAC, as detected by a specific antibody for C5b-9 complex (Fig. 1B). In this respect LAL behaves very similarly to EOMs, which are primarily affected in MFS (Jacobs et al., 2003). No MAC deposition was observed when FS3 was combined to heat-inactivated NHS (FS3 + HI-NHS), or when muscles were exposed to NHS.

FS3 + NHS, administered subcutaneously in the LAL muscles or in the hind limbs, causes a progressive degeneration of motor axon terminals, monitored by the disappearance of neurofilaments (NF) and VAchT stainings over time (Fig. 2A and B). Maximum degeneration takes place in LAL muscles after 24 h treatment, with 61% NMJs lacking NF and VAchT stainings (144 NMJs analyzed, 3 independent experiments), and after 48 h in soleus muscles with 92% of degenerated NMJs (137 NMJs analyzed, 3 independent experiments). Strikingly, few days post-injection motor axon terminals regrow completely, in line with the known reversibility of MFS. NMJ functional recovery was quantitatively estimated in soleus muscles by electrophysiology (Fig. 2C). Neurotransmission is compromised at 48 h, but is restored within

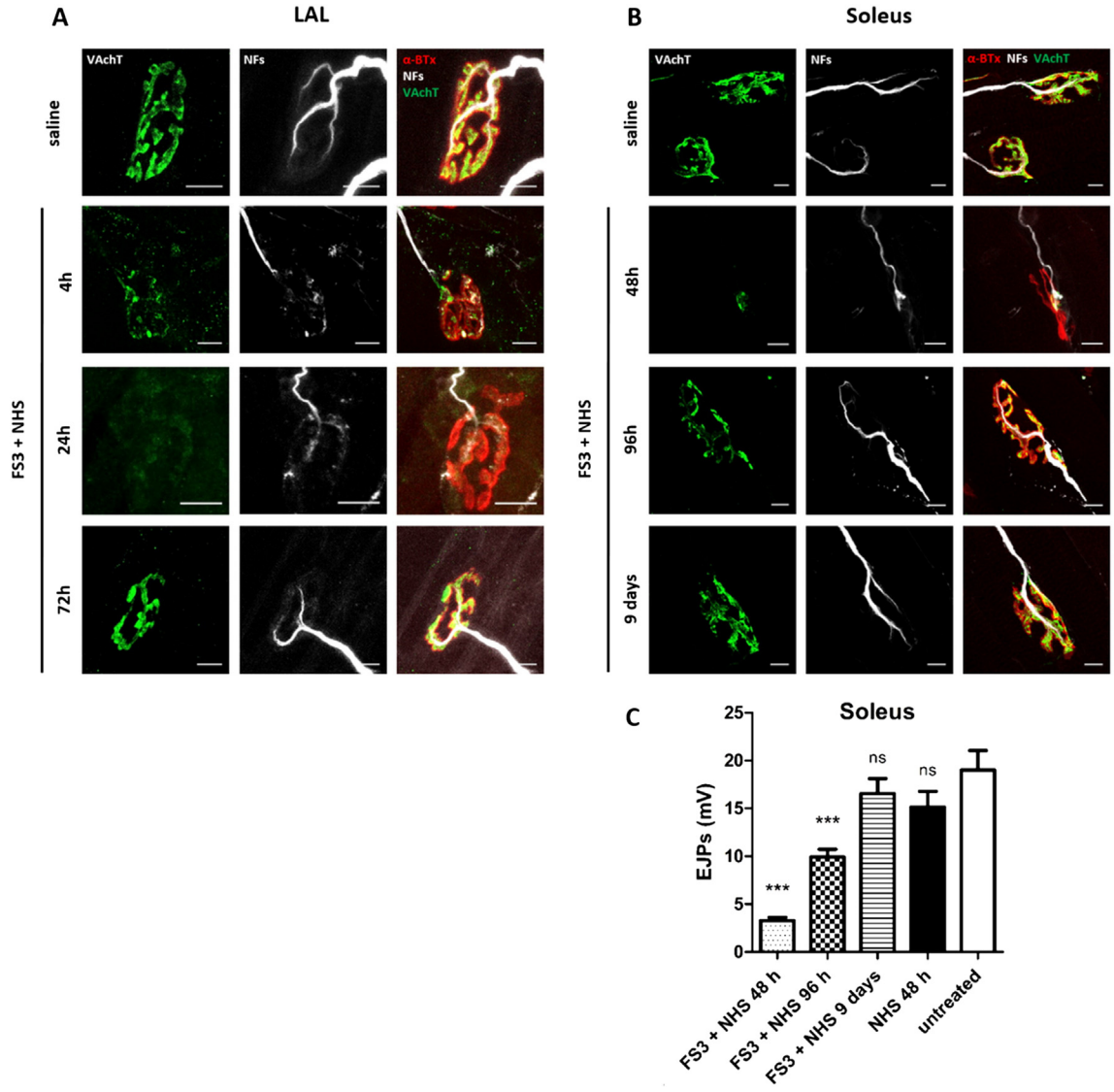

Fig. 2. Anti-GQ1b *plus* complement triggers a reversible nerve terminal degeneration *in vivo* at murine NMJs. Kinetics of VAchT and NF loss (*green* and *white* respectively) in LAL (A) and soleus (B) NMJs following injection of FS3 + NHS, and subsequent recovery. The postsynaptic element is stained by fluorescent α-BTx (*red*). Scale bars: 10 μm. (C) EJPs were recorded in soleus muscles upon local injection of FS3 + NHS, NHS or saline for the indicated time points. Bars represent the average EJP amplitude of 45 muscle fibres from 3 different mice per time point. Student's unpaired *t*-test, two-sides, $^{***}p < 0.0001$ *versus* control (vehicle). Error bars represent SEM, ns = not significant.

9 days, in line with immunofluorescence results. No degeneration is induced by administration of NHS or of FS3 + HI-NHS (Figs. 2C and S1).

3.2. Anti-GQ1b antibody binds specifically to primary neurons and triggers MAC assembly on neuronal surface in the presence of complement

To gain insights into the molecular mechanisms underpinning nerve terminal degeneration and regeneration induced by FS3 + NHS we moved to an *in vitro* model, consisting of primary neuronal cultures from the cerebellum or from the spinal cord. Cerebellar granular neurons (CGNs) are an almost pure neuronal population (Levi et al., 1984), whilst spinal cord motor neurons (SCMNs) are those most related to peripheral motor neurons, and are a mixed culture (Arce et al., 1999).

FS3 binds specifically to neurons (β_3-tubulin positive cells), and no staining was observed either in the non-neuronal cells of the SCMNs preparation or in primary SCs (Fig. 3A). Interestingly, FS3 staining is not uniform, as it appears enriched in discrete domains of the plasma membrane. Likely, this localization may be related to the distribution in patches of neuronal polysialogangliosides, together with sphingolipids and cholesterol (Aureli et al., 2015).

FS3 + NHS triggers MAC deposition on the surface of SCMNs (Fig. 3B). At the site of MAC localization, *bulges* or varicosities develop very rapidly (arrowheads, panels at higher magnitude). Similar results were obtained in CGNs (Fig. S2A). No *bulges* nor MAC deposition occur upon FS3 + HI-NHS or NHS exposure (Figs. 3B and S2A).

3.3. MAC assembly mediates Ca^{2+} entry into neurons

The activation of the complement cascade leads to MAC formation, with consequent extracellular Ca^{2+} influx, as shown by Ca^{2+} *imaging* experiments performed both in SCMNs (Fig. 4A and Supplementary movie S1) and in CGNs (Fig. S3A and Supplementary movie S3). No intracellular calcium concentration ($[Ca^{2+}]_i$) changes take place either upon FS3 + HI-NHS exposure or with NHS(Figs. 4A and S3A and Supplementary movies S2, S4). The intracellular calcium rise is particularly relevant within *bulges* and neurites (Figs. 4B and S3B). Neuronal *bulging* is likely to be driven, at least in part, from the osmotic imbalance due to large proteins and other osmotically active intracellular components, that cannot permeate through the complement pore, whose internal diameter has been estimated in the order of 10 nm (Aleshin et al., 2012; Serna et al., 2016). Neuronal *bulging* also occurs in primary neurons exposed to spider and snake neurotoxins, which cause a degeneration of nerve terminals mainly due to a toxic Ca^{2+} overload. Such *bulges* are at least in part the result of an unbalanced exo-endocytosis, and are sites of vesicular markers accumulation (Tedesco et al., 2009). MAC was found to accumulate within *bulges* (Fig. 3B), and in treated neurons FS3 partially co-localizes with the vesicular protein VAMP2 (vesicle associated membrane protein 2, Fig. S2B), suggesting a possible contribution of altered synaptic vesicle recycling to the development of *bulges*.

3.4. Anti-GQ1b antibody plus complement causes mitochondrial alterations in cultured neurons

Upon exposure to FS3 + NHS mitochondria of SCMNs lose their elongated shape and accumulate within *bulges* (Fig. 5A), that are sites of calcium overload. Mitochondria have been reported to migrate toward cellular sites where calcium levels are increased, in order to buffer it (Yi et al., 2004). Mitochondria within *bulges* are dysfunctional, as they loose with time the ability to retain the membrane potential indicator TMRM dye (Fig. 5B,C). TMRM is accumulated within the mitochondrial matrix due to the negative membrane potential across the inner membrane of these organelles. No morphological nor functional changes took place upon treatment with HI-NHS or NHS. Similar results were obtained in CGNs (Fig. S4). These findings indicate that anti-GQ1b antibody *plus* complement represents a defined pathological effector capable of affecting calcium and mitochondria homeostasis in neurons.

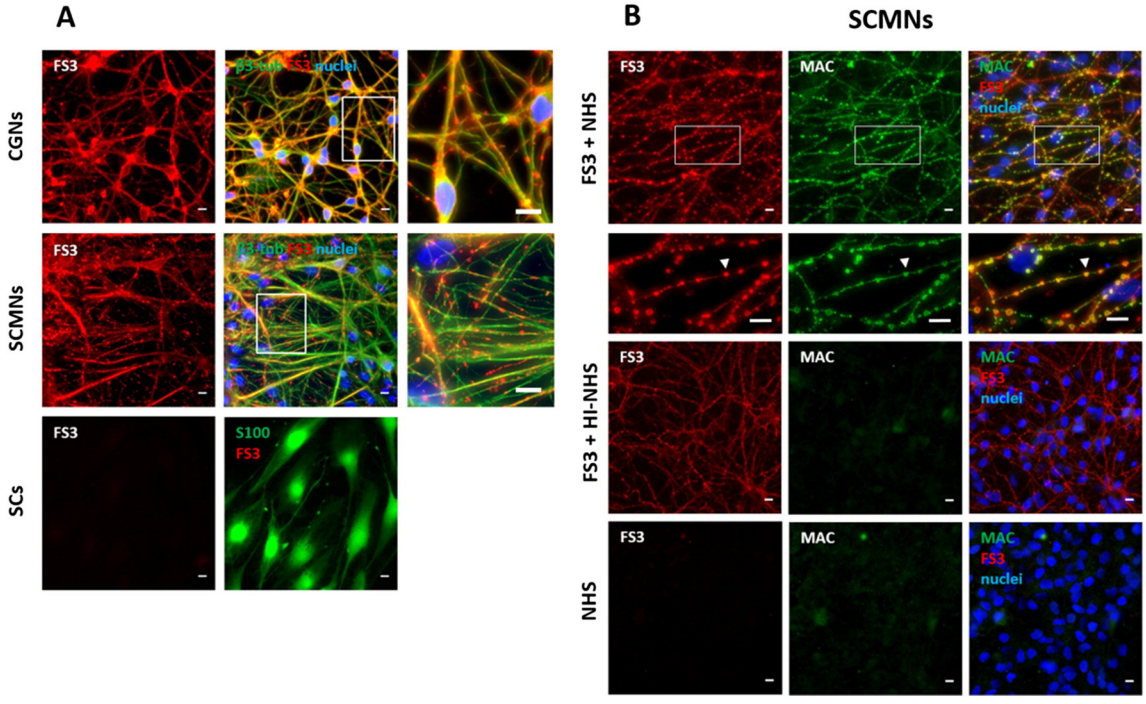

Fig. 3. Anti-GQ1b binding and MAC deposition in primary neurons. (A) FS3 (*red*) binding to both CGNs and SCMNs (β_3-tubulin positive, *green*) after 20 min incubation at 16 °C. FS3 punctuated staining is restricted to neuronal cells, as no signal is detectable in SCs (identified by S100 labeling, *green*, lower panel). Nuclei are stained by Hoechst (*blue*). Scale bar: 10 μm. (B) FS3 + NHS triggers MAC deposition and *bulge* formation in SCMNs upon 20 min incubation at 37 °C. MAC (*green*) co-localizes with FS3 (*red*) at neuronal *bulges* (*arrowheads*). FS3 + HI-NHS or NHS fail to trigger MAC deposition. Nuclei are stained by Hoechst. Scale bars: 10 μm.

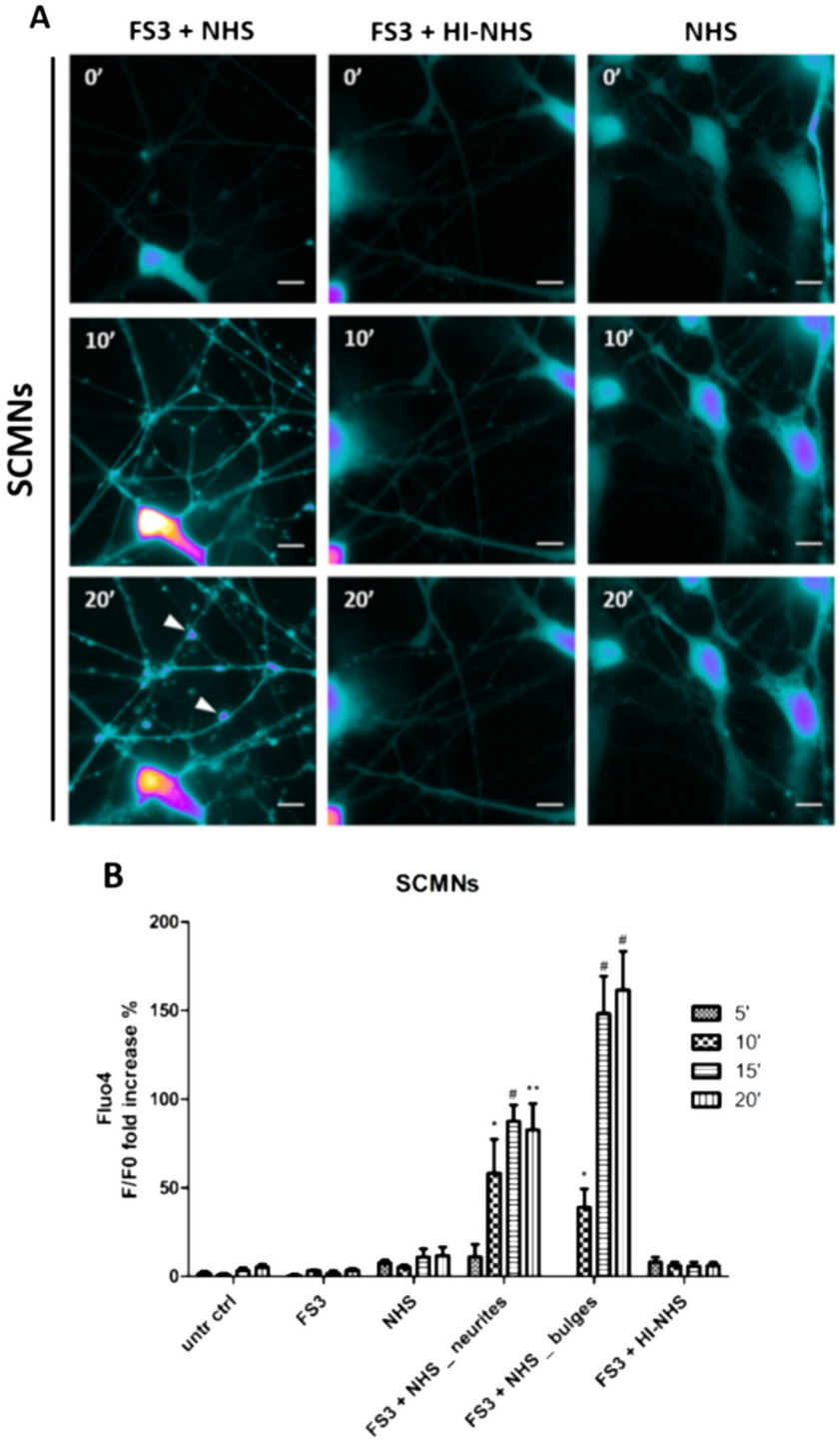

Fig. 4. Anti-GQ1b *plus* complement induces Ca^{2+} influx in cultured neurons. (A) SCMNs loaded with Fluo-4 AM were exposed to FS3 + NHS, FS3 + HI-NHS, NHS or FS3 (not shown) for 20 min, and intracellular [Ca^{2+}] calcium changes monitored over time. Images are presented in pseudocolors (*blue*, low calcium; *white*, high calcium). Scale bars: 10 μm. (B) Quantification of selected ROI in correspondence of neurites is shown. In FS3 + NHS samples also ROI within *bulges* have been measured. N = 3, Student's unpaired *t*-test, two-sides, $^{*}p < 0.05$, $^{**}p < 0.01$, $^{\#}p < 0.001$.

3.5. Anti-GQ1b antibody plus complement induces mitochondrial hydrogen peroxide production in cultured neurons

High calcium uptake in mitochondria causes the opening of the permeability transition pore and impairs the functionality of the respiratory chain, with production of reactive oxygen species (Rasola and Bernardi, 2011; Giorgio et al., 2013). Superoxide anion is short lived, as it is rapidly reduced by the mitochondrial superoxide dismutases to hydrogen peroxide (H_2O_2) and oxygen (Paulsen and Carroll, 2010). H_2O_2 is more stable and can act as an intercellular signaling molecule, as well as a paracrine mediator on neighboring cells, given its permeation through aquaporin channels (Miller et al., 2010; Bienert and Chaumont, 2014).

To test whether H_2O_2 is produced inside neurons upon FS3 + NHS exposure, cells were loaded with H_2O_2 specific probes with different subcellular localization, PF6-AM (cytoplasmic) and MitoPY1 (mitochondrial)

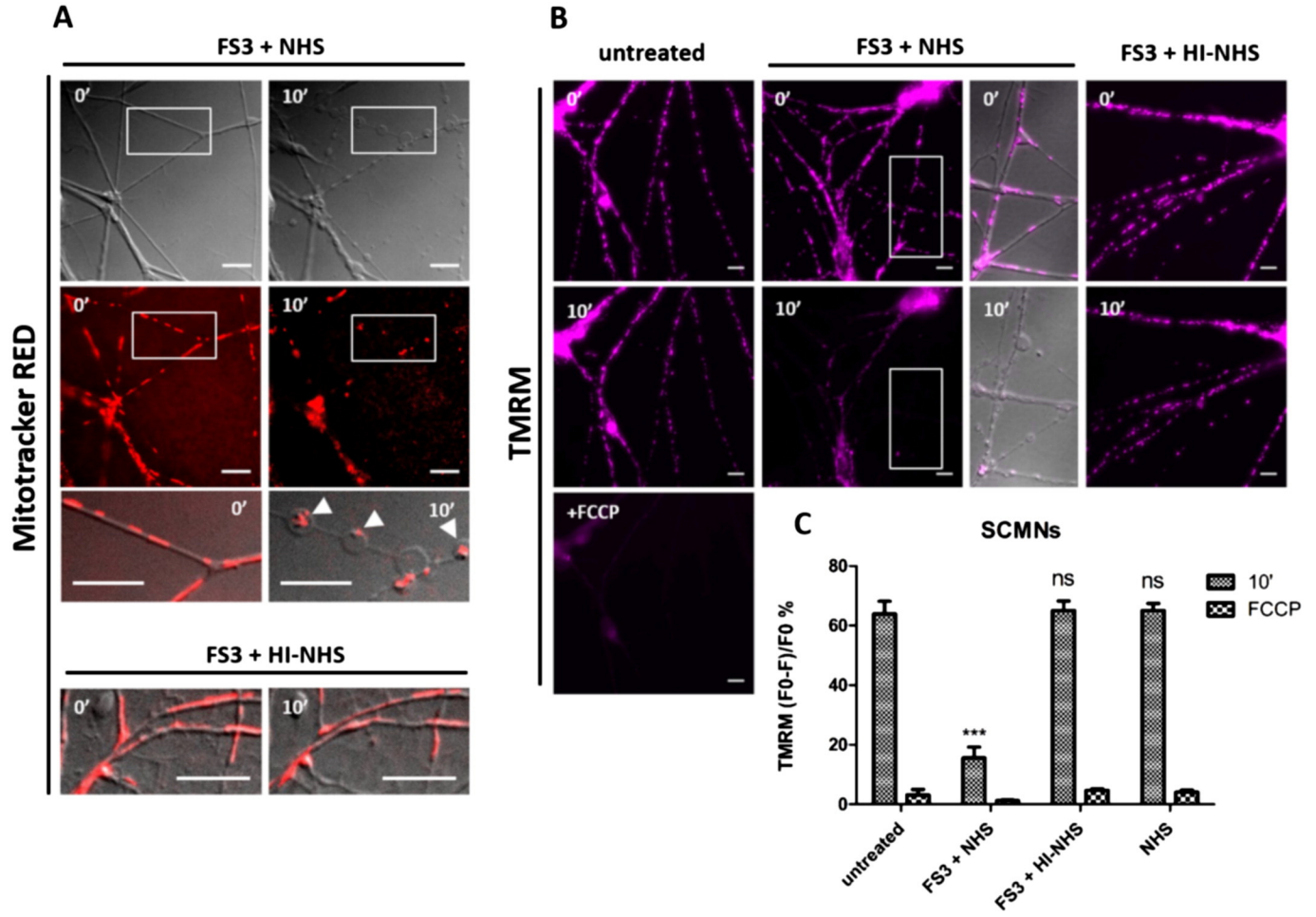

Fig. 5. Anti-GQ1b *plus* complement alters mitochondrial morphology and functionality within cultured neurons. (A) SCMNs were loaded with Mitotracker-Red and exposed to FS3 + NHS for 10 min. Over time mitochondria become rounded and accumulate within *bulges* (arrowheads, lower panels at higher magnification). No changes are detectable when NHS is heat-inactivated. Scale bars: 10 μm. (B) SCMNs loaded with TMRM were exposed for 10 min to saline, FS3 + NHS, FS3 + HI-NHS or NHS. Mitochondria of FS3 + NHS treated neurons progressively loose the dye, indicating an impairment of functionality. No TMRM loss is observed with FS3 + HI-NHS or NHS. The complete loss of TMRM is achieved upon FCCP addition (positive control). Scale bars: 10 μm. Quantification is shown in (C). N = 3, Student's unpaired *t*-test, two-sides, $^{***}p < 0.001$.

(Dickinson et al., 2011; Dickinson and Chang, 2008). FS3 + NHS induces a progressive production of H_2O_2 both in SCMNs and in CGNs (Figs. 6 and S5 respectively) in correspondence of neuronal *bulges* (*arrowheads*). H_2O_2 is produced inside mitochondria, as revealed by MitoPY1 loading of CGNs (Fig. 6C). No H_2O_2 production is detected upon FS3 + HI-NHS or NHS exposure. Noticeably, calcium increase and H_2O_2 generation spatially and temporally correlate, suggesting that the two phenomena are biochemically connected.

3.6. Neuronal hydrogen peroxide triggers ERK 1/2 phosphorylation in Schwann cells

Growing evidence indicate that H_2O_2 is an important intercellular signaling molecule regulating kinase-driven pathways (Gough and Cotter, 2011; Murphy et al., 2011). It triggers ERK phosphorylation in different cell types with consequent activation of downstream gene transcription. Phospho-ERK and phospho-c-jun signaling pathways were recently shown to play a central role in the orchestration of axon repair by SCs (Napoli et al., 2012; Arthur-Farraj et al., 2012), and ERK1/2 becomes phosphorylated in a model of motor axon terminal injury caused by presynaptic animal neurotoxins (Duregotti et al., 2015). The activated SCs then participate actively to the process of nerve terminal regeneration after NMJ damage (Son et al., 1996).

We therefore tested ERK phosphorylation in co-cultures of primary neurons and primary SCs exposed to FS3 + NHS, and found generation of p-ERK in SCs (Fig. 7). The addition of catalase, a H_2O_2-inactivating enzyme, in the extracellular medium largely reduced ERK phosphorylation in SCs, indicating an important contribution of H_2O_2 to ERK activation. No p-ERK increase was detected neither in isolated neurons nor in neurons in co-cultures upon exposure to FS3 + NHS. FS3 + HI-NHS or NHS fail to trigger any ERK phosphorylation in co-cultured SCs.

4. Discussion

Here we have used a mouse monoclonal anti-antibody (FS3), specific toward the polysialogangliosides GQ1b and GT1a, raised against the same pathogen (*Campylobacter jejuni*) that had generated autoimmune antibodies in an MFS patient (Koga et al., 2005). We combined this specific antibody with amounts of complement which were chosen after a careful evaluation of a range of complement concentrations. This is an important preliminary point since large amounts of sera cause a variety of artifacts in cultured neurons and at the NMJ. The combination of FS3 *plus* complement represents the '*pathogen*' responsible for the MFS peripheral autoimmune neuropathy.

In the presence of a complement source, autoantibody binding to neuronal membranes leads to MAC deposition, with appearance of *bulges* along neurites, where $[Ca^{2+}]_i$ increases. This triggers

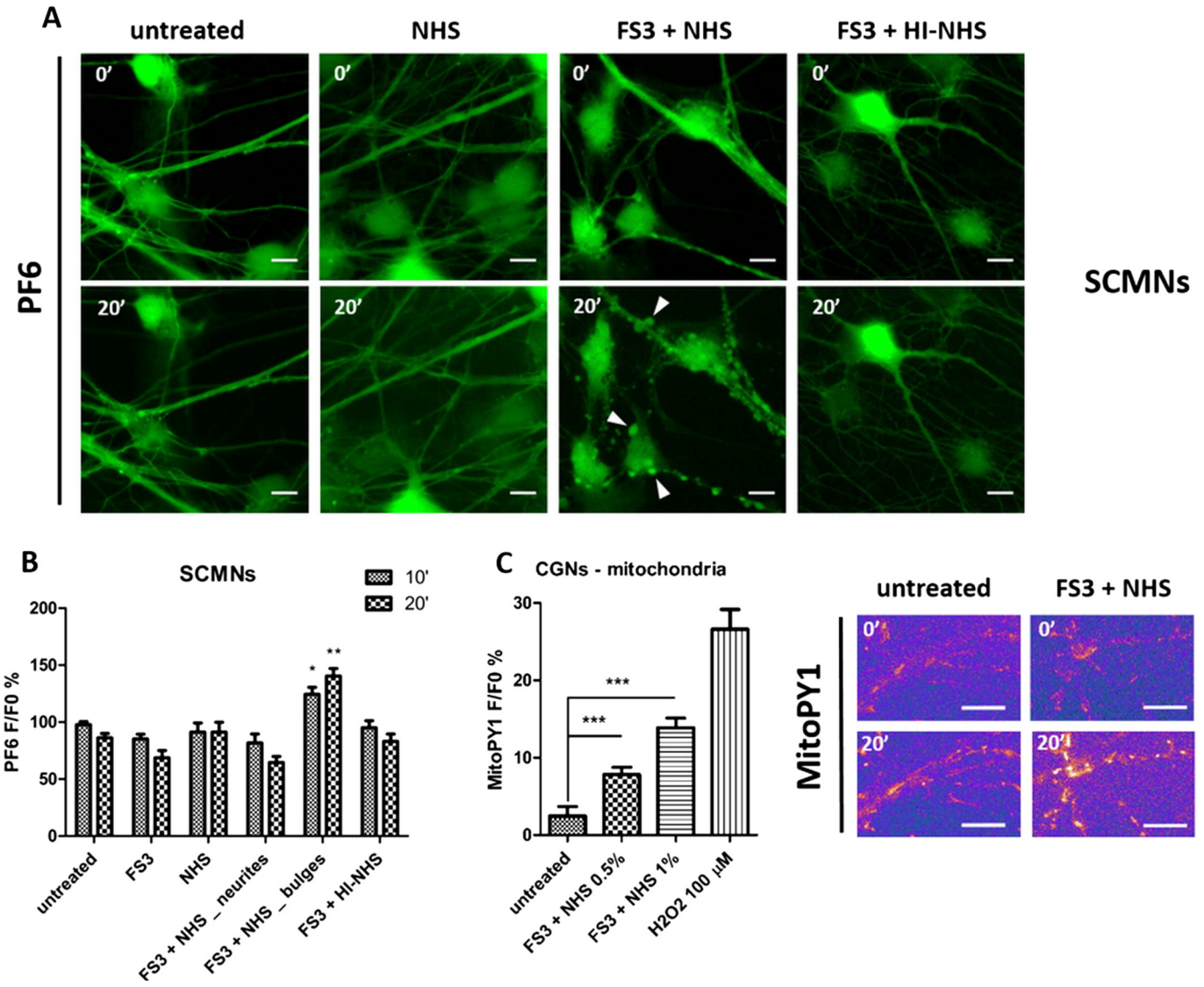

Fig. 6. Anti-GQ1b *plus* complement triggers hydrogen peroxide production in primary neurons. (A) SCMNs loaded with the H_2O_2 probe PF6-AM were exposed to saline, FS3 + NHS, NHS, FS3 + HI-NHS, or to FS3 (not shown) for 20 min, and changes in fluorescence were measured over time. Scale bar: 10 μm. Quantification of H_2O_2 production at the level of neurites and *bulges* (*arrowheads*) is shown (B). N ≥ 4 independent experiments for each condition, Student's unpaired *t*-test, two-sides, $^{*}p < 0.05$, $^{**}p < 0.01$. (C) Hydrogen peroxide is produced inside mitochondria of CGNs loaded with the mitochondrial probe MitoPY1. Hydrogen peroxide (100 μM) was used as positive control. N = 3, Student's unpaired *t*-test, two-sides, $^{\#}p < 0.001$.

accumulation of mitochondria that exhibit loss of the normal structure and function. These dysfunctional mitochondria produce H_2O_2, which diffuses outside neurons and permeates into neighboring SCs, activating the MAPK pathway within these cells.

Impairment of the respiratory chain functionality caused by mitochondrial Ca^{2+} accumulation leads to a largely increased production of reactive oxygen species (ROS), in particular of superoxide anions, that are rapidly converted into H_2O_2 (Paulsen and Carroll, 2010). This molecule has been detected in mitochondria using a specific probe, which accumulates within the mitochondrial matrix, and becomes fluorescent upon peroxidation (Dickinson and Chang, 2008).

H_2O_2 has been commonly included among ROS, harmful molecules which damage cell components owing to their oxidant activity. However, increasing evidence indicate that H_2O_2 is also an intercellular signaling mediator involved in variety of events, including leukocyte recruitment into inflammatory sites (Niethammer et al., 2009) and organ regeneration in tadpoles (Love et al., 2013). The present paper documents the novel finding that neuronal H_2O_2, released from degenerating neurons attacked by the combination of autoantibodies and complement, is capable of inducing ERK1/2 signaling in co-cultured SCs, and this effect is strongly reduced by the presence of extracellular catalase, which inactivates H_2O_2 during its diffusion from neurons to SCs.

These results are reminescent of those obtained during the nerve terminal degeneration induced by some animal neurotoxins, which also induce cytosolic $[Ca^{2+}]_i$ increase (Rigoni et al., 2007, 2008; Duregotti et al., 2015). In many forms of neuronal damages the MAPK pathway participates in the activation of SCs during nerve regeneration (Jessen et al., 2015). Remarkably, here the addition of catalase to the extracellular medium largely reduces ERK activation in SCs, proving that H_2O_2 migrates out of the damaged nerve terminals toward SCs and triggers the activation of the MAPK pathway. Catalase does not completely abolish such signaling activation: in fact other inter-cellular signaling molecules are believed to be released by the degenerating nerve terminals. It has been reported that the engagement of the HIF-1a-erythropoietin signaling, triggered by the release of nitric oxide from injured axons, protects against axonal degeneration (Keswani et al., 2011).

We are planning to identify the additional *alarm* signals released by damaged nerve terminals, as well as mediators produced by PSCs and by muscle fibres to induce and drive the motor axon to regrow toward its original site, to reform a functional NMJ.

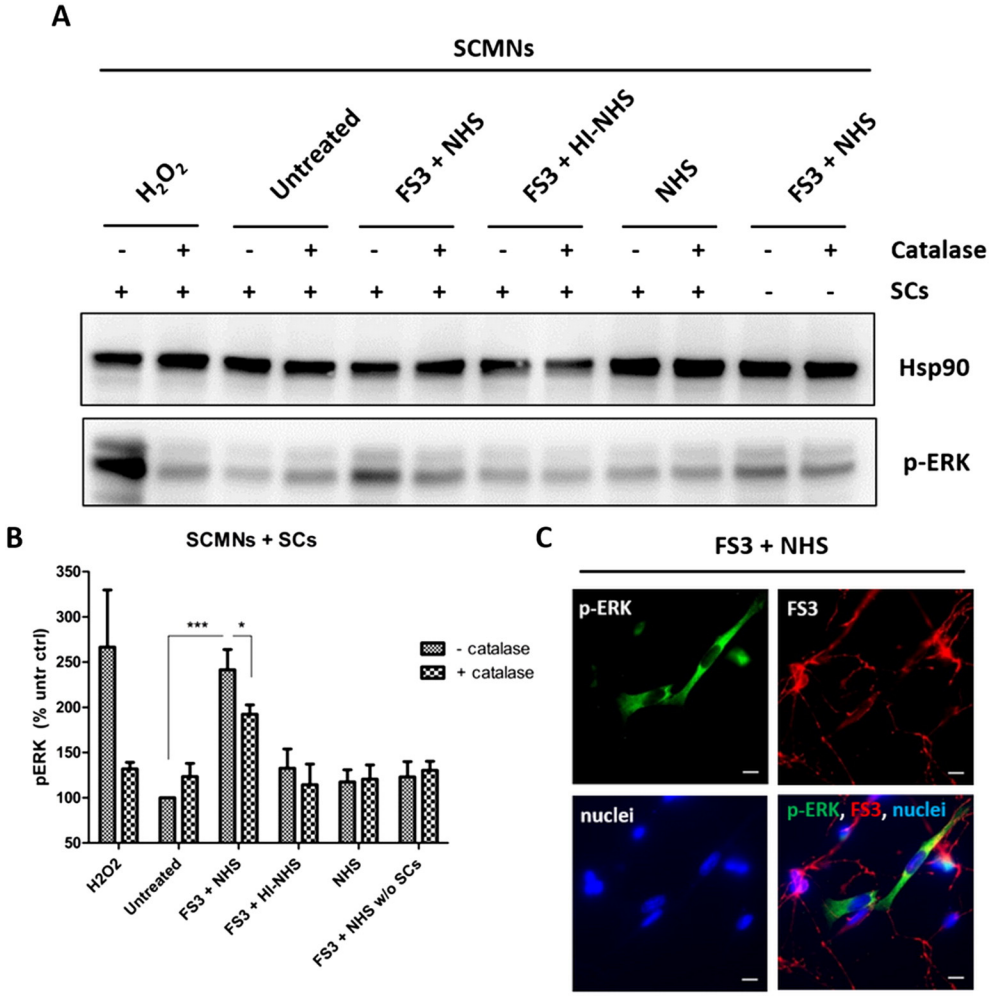

Fig. 7. Anti-GQ1b *plus* complement induces ERK1/2 phosphorylation in SCs co-cultured with neurons. (A) Representative Western blot showing ERK phosphorylation induced by 30 min incubation with FS3 + NHS in SCs co-cultured with SCMNs. Phospho-ERK levels are reduced upon pre-incubation with catalase. No ERK activation is detected following exposure to NHS or when NHS is heat-inactivated. FS3 + NHS fails to increase p-ERK levels in isolated SCMNs. (B) Quantification of p-ERK levels normalized on Hsp90 signal. N = 5, Student's unpaired *t*-test, two-sides, $^{*}p < 0.05$, $^{***}p < 0.001$. (C) Phospho-ERK signal (*green*) is restricted to SCs in neurons-SCs co-cultures treated with FS3 + NHS for 30 min, in line with Western blot results. Neurons are detectable by FS3 staining (*red*). Nuclei are stained by Hoechst (*blue*). Scale bar: 10 μm.

Supplementary data to this article can be found online at http://dx.doi.org/10.1016/j.nbd.2016.09.005.

Acknowledgments

This work was supported by the Cariparo Foundation "Synaptic Functions and Role of Glial Cells in Brain and Muscle Diseases" (to C.M.) and the "University of Padua" 3-2015 (to M.R.). C.J.C. is an Investigator with the Howard Hughes Medical Institute and thanks NIH (GM79465) for support. B.C.D. was partially supported by a Chemical Biology Interface Training Grant from the NIH (T32 GM066698).

References

Aleshin, A.E., et al., 2012. Structure of complement C6 suggests a mechanism for initiation and unidirectional, sequential assembly of membrane attack complex (MAC). J. Biol. Chem. 287, 10210–10222.
Angaut-Petit, D., et al., 1987. The *levator auris longus* muscle of the mouse: a convenient preparation for studies of short- and long-term presynaptic effects of drugs or toxins. Neurosci. Lett. 82, 83–88.
Arce, V., et al., 1999. Cardiotrophin-1 requires LIFRbeta to promote survival of mouse motoneurons purified by a novel technique. J. Neurosci. Res. 55, 119–126.
Arthur-Farraj, P.J., et al., 2012. c-Jun reprograms Schwann cells of injured nerves to generate a repair cell essential for regeneration. Neuron 75, 633–647.
Aureli, M., et al., 2015. Lipid membrane domains in the brain. Biochim. Biophys. Acta 1851, 1006–1016.
Bano, D., Nicotera, P., 2007. Ca^{2+} signals and neuronal death in brain ischemia. Stroke 38, 674–676.
Bienert, G.P., Chaumont, F., 2014. Aquaporin-facilitated transmembrane diffusion of hydrogen peroxide. Biochim. Biophys. Acta 840, 1596–1604.
Chiba, A., et al., 1993. Serum anti-GQ1b IgG antibody is associated with ophthalmoplegia in Miller Fisher syndrome and Guillain-Barrè syndrome: clinical and immunohistochemical studies. Neurology 43, 1911–1917.
Dickinson, B.C., Chang, C.J., 2008. A targetable fluorescent probe for imaging hydrogen peroxide in the mitochondria of living cells. J. Am. Chem. Soc. 130, 9638–9639.
Dickinson, B.C., et al., 2011. Nox2 redox signaling maintains essential cell populations in the brain. Nat. Chem. Biol. 7, 106–112.
Duregotti, E., et al., 2015. Mitochondrial alarmins released by degenerating motor axon terminals activate perisynaptic Schwann cells. Proc. Natl. Acad. Sci. U. S. A. 112, E497–E505.
Fisher, C.M., 1956. An unusual variant of acute idiopathic polyneuritis (syndrome of ophthalmolplegia, ataxia and areflexia). N. Engl. J. Med. 255, 57–65.
Giorgio, V., et al., 2013. Dimers of mitochondrial ATP synthase form the permeability transition pore. Proc. Natl. Acad. Sci. U. S. A. 110, 5887–5892.
Goodyear, C.S., et al., 1999. Monoclonal antibodies raised against Guillain-Barré syndrome-associated *Campylobacter jejuni* lipopolysaccharides react with neuronal gangliosides and paralyze muscle-nerve preparations. J. Clin. Invest. 104, 697–708.
Gough, D.R., Cotter, T.G., 2011. Hydrogen peroxide: a Jekyll and Hyde signalling molecule. Cell Death Dis. 2, e213.
Halstead, S.K., et al., 2004. Anti-disialoside antibodies kill perisynaptic Schwann cells and damage motor nerve terminals via membrane attack complex in a murine model of neuropathy. Brain 127, 2109–2123.
Jacobs, B.C., et al., 2003. Immunoglobulins inhibit pathophysiological effects of anti-GQ1b-positive sera at motor nerve terminals through inhibition of antibody binding. Brain 126, 2220–2234.

Jessen, K.R., et al., 2015. Schwann cells: development and role in nerve repair. Cold Spring Harb. Perspect. Biol. 7, a020487.
Keswani, S.C., et al., 2011. Nitric oxide prevents axonal degeneration by inducing HIF-1-dependent expression of erythropoietin. Proc. Natl. Acad. Sci. U. S. A. 108, 4986–4990.
Koga, M., et al., 2005. Antecedent infections in Fisher syndrome: a common pathogenesis of molecular mimicry. Neurology 64, 1605–1611.
Levi, G., et al., 1984. Autoradiographic localization and depolarization-induced release of acidic amino acids in differentiating cerebellar granule cell cultures. Brain Res. 290, 77–86.
Liu, J.X., et al., 2009. Immunolocalization of GQ1b and related gangliosides in human extraocular neuromuscular junctions and muscle spindles. Invest. Ophthalmol. Vis. Sci. 50, 3226–3232.
Love, N.R., et al., 2013. Amputation-induced reactive oxygen species are required for successful Xenopus tadpole tail regeneration. Nat. Cell Biol. 15, 222–228.
Miller, E.W., et al., 2010. Aquaporin-3 mediates hydrogen peroxide uptake to regulate downstream intracellular signaling. Proc. Natl. Acad. Sci. U. S. A. 107, 15681–15686.
Murphy, M.P., et al., 2011. Unraveling the biological roles of reactive oxygen species. Cell Metab. 13, 361–366.
Napoli, I., et al., 2012. A central role for the ERK-signaling pathway in controlling Schwann cell plasticity and peripheral nerve regeneration in vivo. Neuron 73, 729–742.
Niethammer, P., et al., 2009. A tissue-scale gradient of hydrogen peroxide mediates rapid wound detection in zebrafish. Nature 459, 996–999.
O'Hanlon, G.M., et al., 2001. Anti-GQ1b ganglioside antibodies mediate complement-dependent destruction of the motor nerve terminal. Brain 124, 893–906.
Orrenius, S., et al., 2003. Regulation of cell death: the calcium-apoptosis link. Nat. Rev. Mol. Cell Biol. 4, 552–565.
Paulsen, C.E., Carroll, K.S., 2010. Orchestrating redox signaling networks through regulatory cysteine switches. ACS Chem. Biol. 5, 47–62.
Rasola, A., Bernardi, P., 2011. Mitochondrial permeability transition in Ca(2+)-dependent apoptosis and necrosis. Cell Calcium 50, 222–233.
Rigoni, M., et al., 2007. Calcium influx and mitochondrial alterations at synapses exposed to snake neurotoxins or their phospholipid hydrolysis products. J. Biol. Chem. 282, 11238–11245.
Rigoni, M., et al., 2008. Snake phospholipase A2 neurotoxins enter neurons, bind specifically to mitochondria, and open their transition pores. J. Biol. Chem. 283, 34013–34020.
Rossetto, O., et al., 1996. VAMP/synaptobrevin isoforms 1 and 2 are widely and differentially expressed in nonneuronal tissues. J. Cell Biol. 132, 167–179.
Rupp, A., et al., 2012. Motor nerve terminal destruction and regeneration following anti-gangliosideantibody and complement-mediated injury: an in and ex vivo imaging study in the mouse. Exp. Neurol. 233, 836–848.
Serna, M., et al., 2016. Structural basis of complement membrane attack complex formation. Nat. Commun. 7, 1–22.
Son, Y.J., et al., 1996. Schwann cells induce and guide sprouting and reinnervation of neuromuscular junctions. Trends Neurosci. 19, 280–285.
Tedesco, E., et al., 2009. Calcium overload in nerve terminals of cultured neurons intoxicated by alpha-latrotoxin and snake PLA2 neurotoxins. Toxicon 54, 138–144.
Wakerley, B.R., et al., 2014. GBS Classification Group; GBS Classification Group. Guillain-Barré and Miller Fisher syndromes—new diagnostic classification. Nat. Rev. Neurol. 9, 537–544.
Yi, M., et al., 2004. Control of mitochondrial motility and distribution by the calcium signal: a homeostatic circuit. J. Cell Biol. 167, 661–672.
Yuki, N., et al., 1994. Molecular mimicry between GQ1b ganglioside and lipopolysaccharides of *Campylobacter jejuni* isolated from patients with Fisher's syndrome. Ann. Neurol. 36, 791–793.